



Article

# Is Upregulation of Aquaporin 4-M1 Isoform Responsible for the Loss of Typical Orthogonal Arrays of Particles in Astrocytomas?

Petra Fallier-Becker <sup>1</sup>, Maike Nieser <sup>1,\*</sup>, Ulrike Wenzel <sup>1</sup>, Rainer Ritz <sup>2</sup> and Susan Noell <sup>3</sup>

<sup>1</sup> Institute of Pathology and Neuropathology, University Hospital of Tuebingen, Liebermeisterstr. 8, 72076 Tuebingen, Germany; petra.fallier-becker@med.uni-tuebingen.de (P.F.-B.); ulrike.wenzel@med.uni-tuebingen.de (U.W.)

<sup>2</sup> Department of Neurosurgery, Schwarzwald-Baar Klinikum, Klinikstr. 11, 78052 Villingen-Schwenningen, Germany; rainer\_ritz@hotmail.com

<sup>3</sup> Department of Neurosurgery, University Hospital of Tuebingen, Hoppe-Seyler-Str. 3, 72076 Tuebingen, Germany; dr.susan.noell@googlemail.com

\* Correspondence: maike.nieser@med.uni-tuebingen.de; Tel.: +49-7071-29-84410

Academic Editor: Kenichi Ishibashi

Received: 13 June 2016; Accepted: 25 July 2016; Published: 29 July 2016

**Abstract:** The astrocytic endfoot membranes of the healthy blood-brain barrier—contacting the capillary—are covered with a large number of the water channel aquaporin 4 (AQP4). They form orthogonal arrays of particles (OAPs), which consist of AQP4 isoform M1 and M23. Under pathologic conditions, AQP4 is distributed over the whole cell and no or only small OAPs are found. From cell culture experiments, it is known that cells transfected only with AQP4-M1 do not form OAPs or only small ones. We hypothesized that in astrocytomas the situation may be comparable to the in vitro experiments expecting an upregulation of AQP4-M1. Quantitative Real-time PCR (qRT-PCR) of different graded astrocytomas revealed an upregulation of both isoforms AQP4 M1 and M23 in all astrocytomas investigated. In freeze fracture replicas of low-grade malignancy astrocytomas, more OAPs than in high-grade malignancy astrocytomas were found. In vitro, cultured glioma cells did not express AQP4, whereas healthy astrocytes revealed a slight upregulation of both isoforms and only a few OAPs in freeze fracture analysis. Taken together, we found a correlation between the decrease of OAPs and increasing grade of malignancy of astrocytomas but this was not consistent with an upregulation of AQP4-M1 in relation to AQP4 M23.

**Keywords:** low-grade astrocytoma; high-grade astrocytoma; malignancy; aquaporin

## 1. Introduction

Aquaporin 4 (AQP4) is the main water channel in the mammalian brain. It is morphologically assembled in square arrays called orthogonal arrays of particles (OAPs) [1–3] localized in superficial and perivascular astrocytic end foot membranes at the blood-brain barrier (BBB). In parenchymal membranes where the astrocyte loses contact to the basal lamina, only a small number of OAPs is found, indicating the polarization of astrocytes [4]. This polarization disappears in astrocytomas. Here, AQP4 protein is strongly upregulated compared to healthy brain tissue as was shown by Saadoun et al. by immunohistological stainings [5]. However, Noell et al. [6] reported that freeze fracture replicas of glioblastomas revealed no or only small OAPs. Western blot analyses of AQP4 expressing cells and tissues revealed two bands for AQP4 that refer to two different AQP4 isoforms: AQP4-M23 and AQP4-M1 with M1 being 22 amino acids (AAs) longer than M23 [7,8]. It is known from in vitro transfection experiments that cells transfected with AQP4-M23-isoform form large lattices of OAPs whereas in M1-transfected cells no or only small OAPs were observed [9,10]. Consequently, we

hypothesized that in astrocytomas, where no typical OAPs have been found in freeze fracture replicas, AQP4-M1 might be upregulated in relation to AQP4-M23. In this work we examined tissues from patients with low-grade to high-grade astrocytomas (World Health Organization (WHO) grade II to IV) asking the question whether or not the AQP4-M1 mRNA is upregulated compared to AQP4-M23 mRNA. Furthermore, we performed freeze fracture analysis of these glioma tissues in order to find out if there is a correlation between the number of OAPs and the grade of malignancy. In addition, cultured glioma cells were analyzed in the same way and compared to normal murine astrocytes in vitro.

## 2. Results

### 2.1. Determination of Orthogonal Arrays of Particles (OAPs) from Low-Grade to High-Grade Malignancies

Using freeze fracture techniques, we analyzed replicas of human astrocytomas from low-grade to high-grade malignancy in order to find out whether or not there is a relationship between the number of typical OAPs and the grade of malignancy of these astrocytomas. Figure 1 shows the freeze fracture replicas of the examined astrocytoma tissues: low-grade astrocytomas (WHO grade II; Figure 1A) revealed membranes with OAPs. The astrocytoma WHO grade III (Figure 1B) showed a few OAPs. IDH1 (isocitrate dehydrogenase 1 (NADP(+))-negative (non-mutated) glioblastomas (Figure 1C) formed only few and sometimes misshapen OAPs or membranes lacking any OAPs.

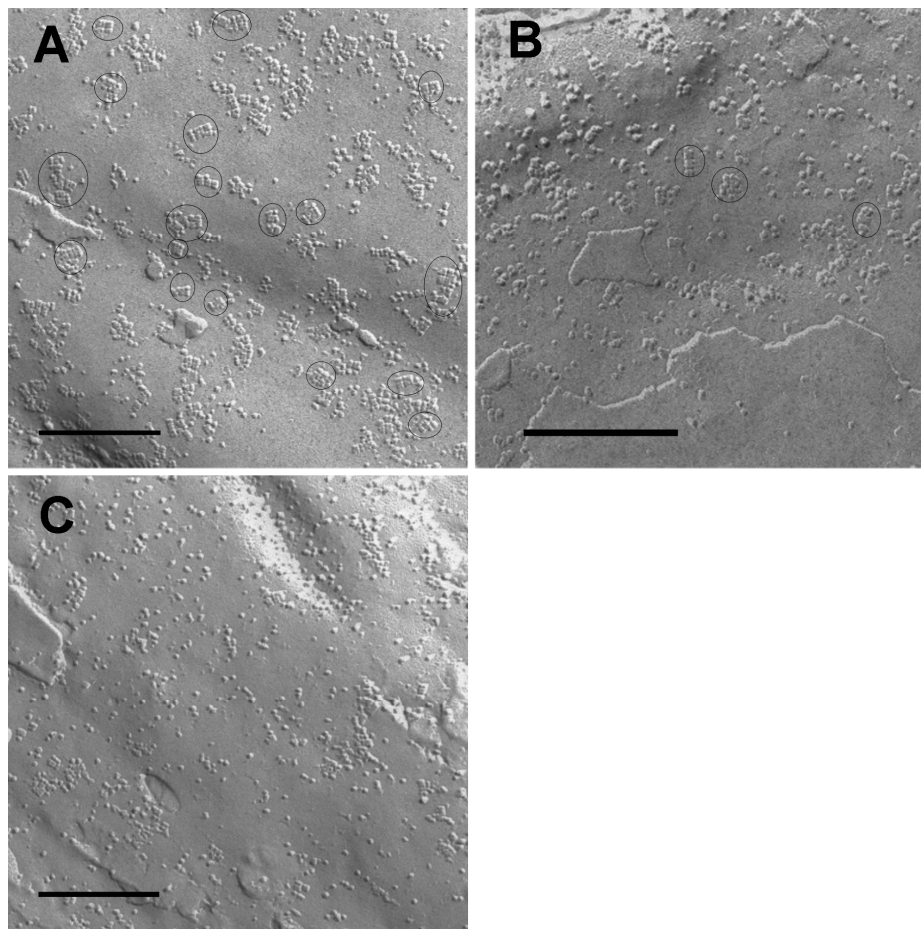


**Figure 1.** Freeze fracture replicas of low-grade to high-grade astrocytomas. (A) Astrocytoma World Health Organization (WHO) grade II showing orthogonal arrays of particles (OAPs) (encircled); (B) Astrocytoma WHO grade III showing less OAPs than in A (encircled); (C) IDH1 (isocitrate dehydrogenase 1 (NADP(+))-negative glioblastoma: No typical OAPs are found. Bar: 250 nm.



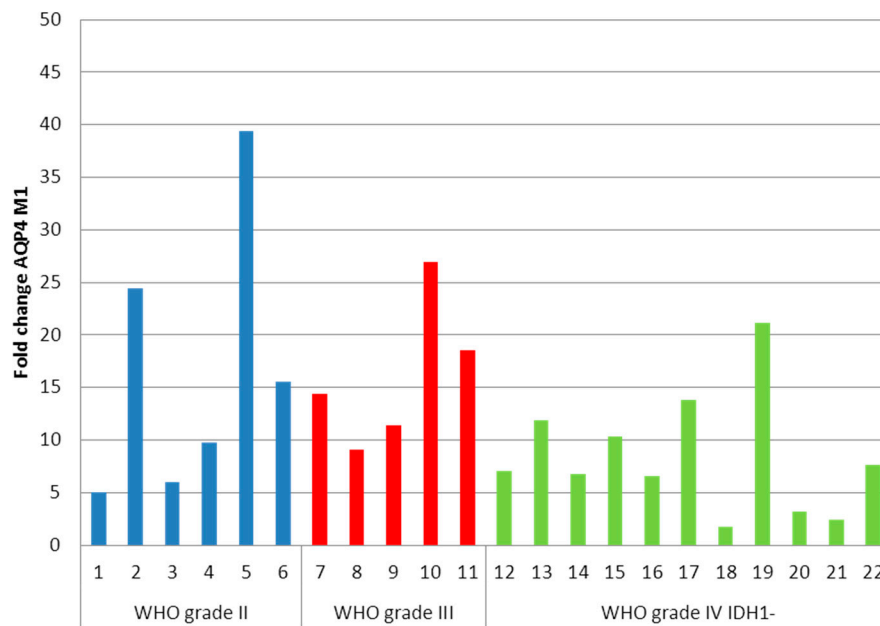


**Figure 3.** Aquaporin 4 (AQP4)-M1 fold changes of astrocytomas. The average fold change is 12.41. No significant differences between the WHO grade groups were detected.

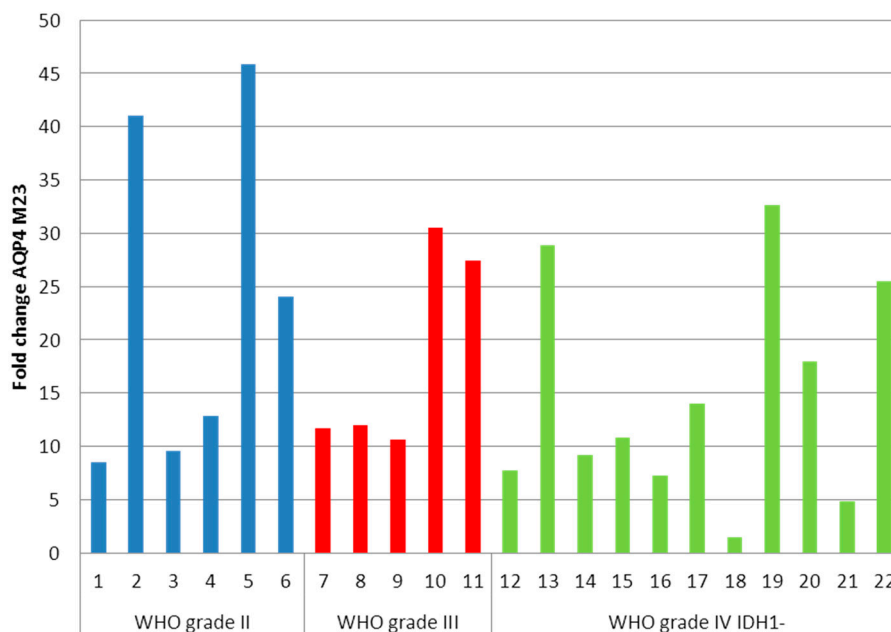


**Figure 4.** AQP4-M23 fold changes of astrocytomas. The average fold change is 17.93. No significant differences between the WHO grade groups were detected.

### 2.3. Determination of AQP4-M1 and -M23 mRNA in Cultures of Normal Astrocytes and Glioma Cells

Cell cultures of murine astrocytes from healthy brain and human glioma cells (TuGlio 25 and U373) were processed for qRT-PCR to compare their expression of AQP4 isoforms to the patients' tumor tissue. Cultured mouse brain astrocytes revealed a slight upregulation of both AQP4-M1 (fold change 4.35) and AQP4-M23X (fold change 4.66, Figure 5) compared to a normal brain. Freeze fracture replicas of mouse astrocytes showed several small sized OAPs (Figure 6).

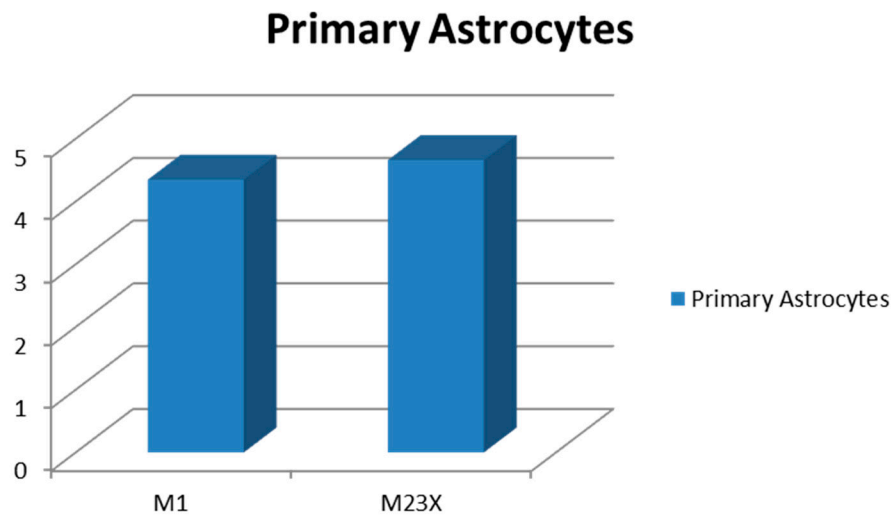


**Figure 5.** AQP4 M1 and M23X fold changes of primary astrocytes. Both isoforms depict 4–5-fold expression compared to the normal mouse brain.

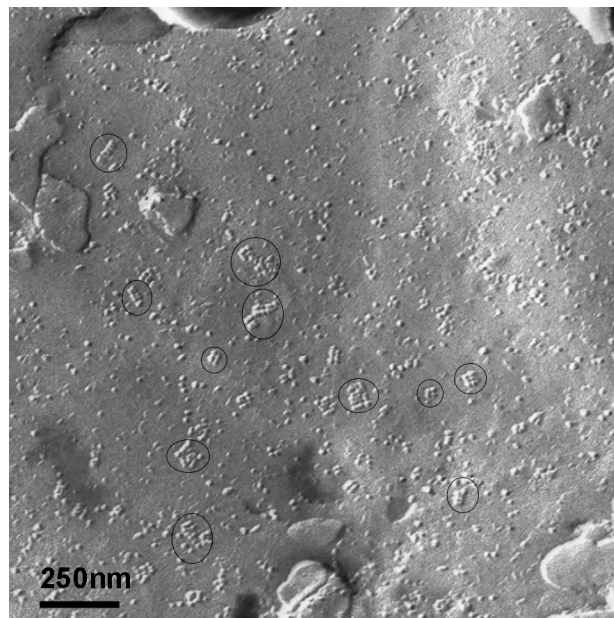


**Figure 6.** Freeze fracture replica of a healthy murine astrocyte in culture showing OAPs encircled.

In U373 and TuGlio25 tumor cells, however, both isoforms were expressed at a very low level (average AQP4-M1 crossing point (CP) values of 32.04 and 34.54 for TuGlio25 and U373, and average AQP4-M23 CP values of 35 and 32.89, respectively) indicating that AQP4 is not expressed in these human tumor cell cultures. Accordingly, no OAPs were formed.

### 3. Discussion

In this work, we furnished proof that the number of OAPs in human astrocytomas decreased from low-grade to high-grade malignancy although the amount of AQP4 protein was increasing [11]. We hypothesized that there might be a connection to the in vitro transfection results of Furman et al. [9] who found no or only small OAPs in AQP4-M1 transfected cell cultures. From these findings, we concluded that astrocytomas revealing no typical OAPs should express more AQP4-M1 than AQP4-M23 compared to the normal brain. However, not only AQP4-M1 but also AQP4-M23 was

upregulated, even to a slightly higher degree than AQP4-M1. Astrocytomas WHO graded II and III depict average  $M23/M1$  ratios of 1.5 and 1.14, whereas the average  $M23/M1$  ratio of glioblastomas is elevated to 1.94. In the healthy brain, however, the  $M23/M1$  is at least 3 [9]. In addition, Jin et al. report that low  $M23/M1$  ratios yield small OAPs, whereas high  $M23/M1$  ratios lead to large OAPs [12]. Our results show that in low-grade and high-grade astrocytomas more AQP4-M23 isoform than AQP4-M1 was expressed despite the decreasing number of OAPs compared to a normal brain. Investigating AQP4-M1 and -M23 mRNA expression of cell cultures of primary tumor cells (TuGlio25) and a tumor cell line (U373) revealed very low AQP4 mRNA expression levels. These results are consistent with the immunohistological investigations of C6 rat glioma cell cultures, which yielded no positive staining for AQP4 [12]. In contrast, in cultures of healthy murine astrocytes, AQP4-M23 and -M1 mRNA were expressed. Here we found the  $M23/M1$  ratio of 1.07 which is comparable to  $M23/M1$  ratios of astrocytomas WHO grade III. In addition, the formation of OAPs in healthy astrocyte cultures was also comparable to the OAPs found in astrocytomas WHO grade II.

Taken together we conclude that loss of OAPs in astrocytomas depends on other factors than the upregulation of AQP4-M1 alone. Former western blot investigations of aquaporin 4 in glioblastoma tissues [6] and rat brain gliomas [13] always yielded the same results: the AQP4-M23 bands were thicker than the M1 bands independent of the formation of OAPs in the appropriate membranes. It seems that the formation of OAPs underlies other mechanisms than change of the  $M23/M1$  ratio. As reported previously, the microenvironment of brain tumors differs from that of normal brains [6]. Our previous findings revealing a correlation between the presence of agrin in the extracellular matrix and the formation of OAPs in glioblastoma and agrin knock-out mice [6,14] suggest that this is also the case in astrocytomas and might be the reason for the decreasing number of OAPs with increasing malignancy of the astrocytomas. In addition to agrin, dystroglycan is also fundamental in forming OAPs. It links agrin in the extracellular matrix via utrophin to alpha syntrophin and to AQP4 [15]. Although investigation of subependymomas reveals also no expression of agrin and dystroglycan and hence no formation of OAPs, these benign tumors are not comparable to the infiltrating astrocytomas [16]. In addition, the activity of matrixmetalloproteinases MMP2, 9, and 3 play a pivotal role in this scenario: if agrin is cleaved by MMP3 [17]—such as in glioblastoma—no typical OAPs are found and if MMP2 and 9 cleave dystroglycan [18]—such as in glioblastoma—no OAPs are formed as well. All these in vivo investigations suggest that the microenvironment in the brain is more important for the formation of OAPs than the  $M23/M1$  relation (Table 1). Furthermore, in vitro experiments showed that murine astrocyte cultures form more OAPs when growing on agrin-coated surfaces or in agrin-containing culture medium [19,20].

**Table 1.** Comparison of typical features between healthy brain and glioblastoma.

Protein Expression/Protein Complex	Healthy Brain	Glioblastoma
Agryn	+	–
Dystroglycan	+	–
Active MMP3	–	+
Active MMP2/9	–	+
OAPs	+	–

It still remains unclear why AQP4 form OAPs and what their role might be. It has been suggested that AQP4 water channels might have a better adhesion to the neighbored membrane if assembled in square arrays [8,21]; others propose a more effective water exchange when AQP4-molecules are packed in OAPs [22]. The isoform AQP4-M23 is suggested to be the faster water channel because it works more effectively in OAPs [23].

## 4. Materials and Methods

### 4.1. Tissue

Tumor tissues from 22 patients with astrocytoma graded WHO II, III, and IV (Table 2) were analyzed using freeze fracture techniques and qRT-PCR. The ethics committee of the medical faculty of the Eberhard-Karls University of Tuebingen approved the project and patients' consent procedures. The ethics committee waived the need for consent (project no. 663/2013BO2). All patients were treated in the Department of Neurosurgery Tuebingen between 2013 and 2014 (Table 2).

**Table 2.** World Health Organization (WHO) grading and IDH1 (isocitrate dehydrogenase 1 (NADP(+)) status of patients.

Patient Number	Astrocytoma WHO Grade	IDH1
1	II	IDH1 (R132H) mutation (IDH1+)
2	II	IDH1 R132H) mutation (IDH1+)
3	II	IDH1 (R132H) mutation (IDH1+)
4	II	IDH1 (R132H) mutation (IDH1+)
5	II	IDH1 (R132H) mutation (IDH1+)
6	II	IDH1 (R132H) mutation (IDH1+)
7	III	IDH1 (R132H) mutation (IDH1+)
8	III	IDH1 (R132H) mutation (IDH1+)
9	III	IDH1 (R132H) mutation (IDH1+)
10	III	IDH1 (R132H) mutation (IDH1+)
11	III	IDH1 (R132H) mutation (IDH1+)
12	IV	IDH1 wildtype (IDH1−)
13	IV	IDH1 wildtype (IDH1−)
14	IV	IDH1 wildtype (IDH1−)
15	IV	IDH1 wildtype (IDH1−)
16	IV	IDH1 wildtype (IDH1−)
17	IV	IDH1 wildtype (IDH1−)
18	IV	IDH1 wildtype (IDH1−)
19	IV	IDH1 wildtype (IDH1−)
20	IV	IDH1 wildtype (IDH1−)
21	IV	IDH1 wildtype (IDH1−)
22	IV	IDH1 wildtype (IDH1−)

### 4.2. Cell Culture

Human primary glioma cells were isolated enzymatically from a patient's glioblastoma. Briefly, resected surgical material was transported under sterile conditions in a 4-(2-hydroxyethyl)-1-piperazineethanesulfonic acid (HEPES) buffered medium (Thermo Fisher Scientific, Waltham, MA, USA) and cells were isolated using trypsin (Sigma, Taufkirchen, Germany). After centrifugation, culture medium was added to the cell pellet and cell suspension was pipetted on a cell strainer (70  $\mu$ m) to get single cells that were seeded in culture flasks and cultured in a humidified incubator at 37 °C and 5% CO<sub>2</sub> under standard conditions with Dulbecco's modified Eagle's medium (DMEM) (Thermo Fisher Scientific, Waltham, MA, USA) supplemented with 10% fetal calf serum (Thermo Fisher Scientific, Waltham, MA, USA), 1% penicillin and streptomycin (Sigma-Aldrich, St. Louis, MO, USA). Culture medium was changed every two days.

Ulrike Naumann, Hertie Institute of Clinical Research, Tuebingen, Germany, kindly provided U373 cells. They were cultured as described above.

Murine cortex astrocytes were isolated from 5 day old mice as described above and cultured under standard conditions [24,25]. When cells reached confluence they were processed for qRT-PCR and freeze fracture analysis.

#### 4.3. Freeze Fracture Technique and Determination of OAP Densities

Tissues and cells were processed for freeze fracture analysis as described before [6].

#### 4.4. RNA Extraction

Cryo tumor specimens of the above-mentioned astrocytomas were gathered from the surgical pathology files of the Department of Neuropathology of the Institute of Pathology of Tuebingen. RNA of the samples and the cell cultures was extracted manually with the RNeasy Mini Kit (Qiagen, Hilden, Germany), following the manufacturer's instructions.

RNA quantification was performed with the NanoDrop ND-2000 (Thermo Fisher Scientific) spectrophotometer.

Human Brain, Cerebral Cortex Total RNA, and Mouse Brain Total RNA (Clontech, Mountain View, CA, USA) served as healthy controls for qRT-PCR.

#### 4.5. cDNA Synthesis

Intron-spanning oligonucleotides for human *HPRT1* (housekeeping gene), *AQP4 M1*, and *AQP4 M23*, as well as murine *Hprt1*, *Aqp4 M1*, and *Aqp4 M23X* [26] were designed using the program Primer3Plus (<http://primer3plus.com/cgi-bin/dev/primer3plus.cgi>). In Tables 3 and 4 the primer sequences and the product sizes are shown. Primer-BLAST (<http://www.ncbi.nlm.nih.gov/tools/primer-blast/>) was used to check for the specificity of the primers.

**Table 3.** Primer (*Homo sapiens*).

Primer	Sequence	Product Size
HPRT1 Ex6 for HPRT1 Ex7 rev	TGACACTGGCAAAACAATGC TTCGTGGGGTCTTTTCACC	101 bp
AQP4 M1 Ex1 for AQP4 M1 Ex2 rev	GGGGAAGGCATGAGTGACAG AAAGCTTGAGTCCAGACCCC	110 bp
AQP4 M23 Ex1 for AQP4 M23 Ex2 rev	TCTCTTTTCAGTAAGTGTGGACCT CATGGCCAGAAATCCGCTG	114 bp

**Table 4.** Primer (*Mus musculus*).

Primer	Sequence	Product Size
HPRT Ex6 Mus for HPRT Ex7 Mus rev	CAAAC TTTGCTTTCCCTGGT GGCCTGTATCCAACACTTCG	91 bp
AQP4 M1 Mus Ex1 for AQP4 M1 Mus Ex2 rev	AGGGAAGGCATGAGTGACAG GACTCCTTTGAAAGCCACCA	96 bp
AQP4 M23X Mus for AQP4 M23X Mus rev	TATGGTTCACGGGTTTGGAT CCCTTTGTCACCTGCTCATT	139 bp

#### 4.6. Quantitative Real Time-PCR (qRT-PCR)

Total RNA (1 µg) was reversely transcribed using the High-Capacity cDNA RT Kit (Thermo Fisher Scientific) in combination with RNA Inhibitor (Thermo Fisher Scientific). The qRT-PCR mix included 10 µL Real-Time SYBR Green PCR master mix, 1 µL (20 ng) diluted reverse transcription product, 2 µL each of Primer (Tables 2 and 3) and 7 µL DNase/RNase free water. The PCR was carried out under following conditions: 95 °C for 15 min followed by 40 cycles of 94 °C for 15 s, 55 °C for 30 s and 70 °C for 30 s in a LightCycler 480 II (Roche, Basel, Switzerland). Normal brain controls as well as a negative water control were included in every run. All samples were run in triplicates.

By running the PCR for 40 cycles, the maximal crossing point (CP) value that could be achieved by the analysis was 35. The CP value is the number of PCR cycles at which a constant fluorescence

level is achieved. CP values between 15 and 25 indicate strong expression, 25–30 medium expression, and >30 weak expression.

To assess the specificity of the amplified PCR product a melting curve analysis was carried out.

#### 4.7. Data Analysis and Statistics

The average raw CP values (median of triplicates) were imported into Microsoft Excel (Version, Microsoft Corp., Seattle, WA, USA). The AQP4-M1 and -M23 expression were analyzed using the comparative  $\Delta$ CP method, where  $\Delta$ CP = CP candidate target – CP reference RNA. HPRT1 was used as endogenous reference gene for the analysis.  $\Delta\Delta$ CP =  $\Delta$ CP sample –  $\Delta$ CP normal brain control, relative expression =  $2^{-\Delta\Delta$ CP}, fold change: if relative expression >1 then fold change  $\hat{=}$  relative expression, if relative expression <1 then fold change =  $-1/\text{relative expression}$ .

M23/M1 ratios were determined by simply dividing the M23 fold changes through the M1 fold changes. For the evaluation of the OAP densities and the AQP4-M1 and -M23 fold changes of the astrocytomas two-tailed unpaired *t*-tests were performed using GraphPad software (Version 4, San Diego, CA, USA). The scatter plot for the OAPs was also achieved by using this software.

## 5. Conclusions

Taken together we were able to demonstrate a significant correlation between the decreasing number of OAPs and the grade of malignancy in human astrocytomas. Furthermore, we found an upregulation of AQP4-M1 as well as an upregulation of -M23 mRNA in all astrocytomas but the M23/M1 ratio differed from 1.14 to 1.5 in low-grade astrocytomas to 1.94 in glioblastomas. These results demand further investigations to elucidate the question whether or not they will yield an impact on the development of new therapeutics.

**Acknowledgments:** We gratefully acknowledge Ria Knittel for preparing the freeze fracture replicas. We are also grateful for Yeliz Donat's excellent technical assistance.

**Author Contributions:** Petra Fallier-Becker and Susan Noell conceived and designed the experiments. Petra Fallier-Becker and Maike Nieser performed the experiments. Petra Fallier-Becker, Susan Noell, Maike Nieser and Ulrike Wenzel analyzed the data. Petra Fallier-Becker, Susan Noell and Maike Nieser wrote the paper. Rainer Ritz provided tumor samples, supervised ongoing experiments and critically revised the manuscript for important intellectual content.

**Conflicts of Interest:** The authors declare no conflict of interest.

## References

1. Rash, J.E.; Yasumura, T.; Hudson, C.S.; Agre, P.; Nielsen, S. Direct immunogold labeling of aquaporin-4 in square arrays of astrocyte and ependymocyte plasma membranes in rat brain and spinal cord. *Proc. Natl. Acad. Sci. USA* **1998**, *95*, 11981–11986. [[CrossRef](#)] [[PubMed](#)]
2. Wolburg, H.; Wolburg-Buchholz, K.; Fallier-Becker, P.; Noell, S.; Mack, A.F. Structure and functions of aquaporin-4-based orthogonal arrays of particles. *Int. Rev. Cell Mol. Biol.* **2011**, *287*, 1–41. [[PubMed](#)]
3. Nicchia, G.P.; Rossi, A.; Mola, M.G.; Pisani, F.; Stigliano, C.; Basco, D.; Mastrototaro, M.; Svelto, M.; Frigeri, A. Higher order structure of aquaporin-4. *Neuroscience* **2010**, *168*, 903–914. [[CrossRef](#)] [[PubMed](#)]
4. Rohlmann, A.; Gocht, A.; Wolburg, H. Reactive astrocytes in myelin-deficient rat optic-nerve reveal an altered distribution of orthogonal arrays of particles (OAP). *Glia* **1992**, *5*, 259–268. [[CrossRef](#)] [[PubMed](#)]
5. Saadoun, S.; Papadopoulos, M.C.; Davies, D.C.; Krishna, S.; Bell, B.A. Aquaporin-4 expression is increased in oedematous human brain tumours. *J. Neurol. Neurosurg. Psychiatry* **2002**, *72*, 262–265. [[CrossRef](#)] [[PubMed](#)]
6. Noell, S.; Wolburg-Buchholz, K.; Mack, A.F.; Ritz, R.; Tatagiba, M.; Beschorner, R.; Wolburg, H.; Fallier-Becker, P. Dynamics of expression patterns of AQP4, dystroglycan, agrin and matrix metalloproteinases in human glioblastoma. *Cell Tissue Res.* **2012**, *347*, 429–441. [[CrossRef](#)] [[PubMed](#)]
7. Neely, J.D.; Christensen, B.M.; Nielsen, S.; Agre, P. Heterotetrameric composition of aquaporin-4 water channels. *Biochemistry* **1999**, *38*, 11156–11163. [[CrossRef](#)] [[PubMed](#)]
8. Smith, A.J.; Jin, B.J.; Ratelade, J.; Verkman, A.S. Aggregation state determines the localization and function of M1- and M23-aquaporin-4 in astrocytes. *J. Cell Biol.* **2014**, *204*, 559–573. [[CrossRef](#)] [[PubMed](#)]

9. Furman, C.S.; Gorelick-Feldman, D.A.; Davidson, K.G.; Yasumura, T.; Neely, J.D.; Agre, P.; Rash, J.E. Aquaporin-4 square array assembly: Opposing actions of M1 and M23 isoforms. *Proc. Natl. Acad. Sci. USA* **2003**, *100*, 13609–13614. [[CrossRef](#)] [[PubMed](#)]
10. Fryer, J.P.; Lennon, V.A.; Pittock, S.J.; Jenkins, S.M.; Fallier-Becker, P.; Clardy, S.L.; Horta, E.; Jedynak, E.A.; Lucchinetti, C.F.; Shuster, E.A.; et al. Aqp4 autoantibody assay performance in clinical laboratory service. *Neuroimmunol. Neuroinflamm.* **2014**, *1*, 1e11. [[CrossRef](#)] [[PubMed](#)]
11. Warth, A.; Simon, P.; Capper, D.; Goeppert, B.; Tabatabai, G.; Herzog, H.; Dietz, K.; Stubenvoll, F.; Ajaaj, R.; Becker, R.; et al. Expression pattern of the water channel aquaporin-4 in human gliomas is associated with blood-brain barrier disturbance but not with patient survival. *J. Neurosci. Res.* **2007**, *85*, 1336–1346. [[CrossRef](#)] [[PubMed](#)]
12. Jin, B.J.; Rossi, A.; Verkman, A.S. Model of aquaporin-4 supramolecular assembly in orthogonal arrays based on heterotetrameric association of M1-M23 isoforms. *Biophys. J.* **2011**, *100*, 2936–2945. [[CrossRef](#)] [[PubMed](#)]
13. Noell, S.; Ritz, R.; Wolburg-Buchholz, K.; Wolburg, H.; Fallier-Becker, P. An allograft glioma model reveals the dependence of aquaporin-4 expression on the brain microenvironment. *PLoS ONE* **2012**, *7*, e36555. [[CrossRef](#)] [[PubMed](#)]
14. Noell, S.; Fallier-Becker, P.; Deutsch, U.; Mack, A.F.; Wolburg, H. Agrin defines polarized distribution of orthogonal arrays of particles in astrocytes. *Cell Tissue Res.* **2009**, *337*, 185–195. [[CrossRef](#)] [[PubMed](#)]
15. Noell, S.; Wolburg-Buchholz, K.; Mack, A.F.; Beedle, A.M.; Satz, J.S.; Campbell, K.P.; Wolburg, H.; Fallier-Becker, P. Evidence for a role of dystroglycan regulating the membrane architecture of astroglial endfeet. *Eur. J. Neurosci.* **2011**, *33*, 2179–2186. [[CrossRef](#)] [[PubMed](#)]
16. Noell, S.; Fallier-Becker, P.; Mack, A.F.; Hoffmeister, M.; Beschorner, R.; Ritz, R. Water channels aquaporin 4 and -1 expression in subependymoma depends on the localization of the tumors. *PLoS ONE* **2015**, *10*, e0131367. [[CrossRef](#)] [[PubMed](#)]
17. Sole, S.; Petegnief, V.; Gorina, R.; Chamorro, A.; Planas, A.M. Activation of matrix metalloproteinase-3 and agrin cleavage in cerebral ischemia/reperfusion. *J. Neuropathol. Exp. Neurol.* **2004**, *63*, 338–349. [[CrossRef](#)] [[PubMed](#)]
18. Agrawal, S.; Anderson, P.; Durbeej, M.; van Rooijen, N.; Ivars, F.; Opdenakker, G.; Sorokin, L.M. Dystroglycan is selectively cleaved at the parenchymal basement membrane at sites of leukocyte extravasation in experimental autoimmune encephalomyelitis. *J. Exp. Med.* **2006**, *203*, 1007–1019. [[CrossRef](#)] [[PubMed](#)]
19. Noell, S.; Fallier-Becker, P.; Beyer, C.; Kroger, S.; Mack, A.F.; Wolburg, H. Effects of agrin on the expression and distribution of the water channel protein aquaporin-4 and volume regulation in cultured astrocytes. *Eur. J. Neurosci.* **2007**, *26*, 2109–2118. [[CrossRef](#)] [[PubMed](#)]
20. Fallier-Becker, P.; Sperveslage, J.; Wolburg, H.; Noell, S. The impact of agrin on the formation of orthogonal arrays of particles in cultured astrocytes from wild-type and agrin-null mice. *Brain Res.* **2011**, *1367*, 2–12. [[CrossRef](#)] [[PubMed](#)]
21. Crane, J.M.; Tajima, M.; Verkman, A.S. Live-cell imaging of aquaporin-4 diffusion and interactions in orthogonal arrays of particles. *Neuroscience* **2010**, *168*, 892–902. [[CrossRef](#)] [[PubMed](#)]
22. Tani, K.; Mitsuma, T.; Hiroaki, Y.; Kamegawa, A.; Nishikawa, K.; Tanimura, Y.; Fujiyoshi, Y. Mechanism of aquaporin-4's fast and highly selective water conduction and proton exclusion. *J. Mol. Biol.* **2009**, *389*, 694–706. [[CrossRef](#)] [[PubMed](#)]
23. Fenton, R.A.; Moeller, H.B.; Zelenina, M.; Snaebjornsson, M.T.; Holen, T.; MacAulay, N. Differential water permeability and regulation of three aquaporin 4 isoforms. *Cell. Mol. Life Sci.* **2010**, *67*, 829–840. [[CrossRef](#)] [[PubMed](#)]
24. Beyer, C.; Raab, H. Nongenomic effects of oestrogen: Embryonic mouse midbrain neurones respond with a rapid release of calcium from intracellular stores. *Eur. J. Neurosci.* **1998**, *10*, 255–262. [[CrossRef](#)] [[PubMed](#)]
25. Ivanova, T.; Karolczak, M.; Beyer, C. Estradiol stimulates GDNF expression in developing hypothalamic neurons. *Endocrinology* **2002**, *143*, 3175–3178. [[CrossRef](#)] [[PubMed](#)]
26. Zelenin, S.; Gunnarson, E.; Alikina, T.; Bondar, A.; Aperia, A. Identification of a new form of AQP4 mRNA that is developmentally expressed in mouse brain. *Pediatr. Res.* **2000**, *48*, 335–339. [[CrossRef](#)] [[PubMed](#)]

